Available online at www.sciencedirect.com
ScienceDirect
Journal of the Mechanics and Physics of Solids 56 (2008) 172–183
JOURNAL OF THE MECHANICS AND PHYSICS OF SOLIDS
www.elsevier.com/locate/jmps

Mechanics of indentation of plastically graded materials—II: Experiments on nanocrystalline alloys with grain size gradients

I.S. Choi[a,b], A.J. Detor[a], R. Schwaiger[b], M. Dao[a], C.A. Schuh[a], S. Suresh[a,*]

[a]*Department of Materials Science and Engineering, Massachusetts Institute of Technology, Cambridge, MA 02139, USA*
[b]*Forschungszentrum Karlsruhe, Institute for Materials Research II, 76344 Karlsruhe, Germany*

Received 8 November 2006; received in revised form 5 July 2007; accepted 6 July 2007

Abstract

A systematic study of depth-sensing indentation was performed on nanocrystalline (nc) Ni–W alloys specially synthesized with controlled unidirectional gradients in plastic properties. A yield strength gradient and a roughly constant Young's modulus were achieved in the nc alloys, using electrodeposition techniques. The force vs. displacement response from instrumented indentation experiments matched very well with that predicted from the analysis of Part I of this paper. The experiments also revealed that the pile-up of the graded alloy around the indenter is noticeably higher than that for the two homogeneous reference alloys that constitute the bounding conditions for the graded material. These trends are also consistent with the predictions of the indentation analysis.

Keywords: Functionally graded materials; Indentation and hardness; Mechanical testing; Nanostructured materials; Numerical algorithms

1. Introduction

The framework for analyzing the mechanics of instrumented indentation in ductile solids with a linear through-thickness variation of yield strength was presented in Part I. Here, we present experimental results that provide direct means to assess the predictions of the indentation analysis by recourse to grain size graded nanocrystalline (nc) alloys with controlled unidirectional gradients in plastic properties and essentially no variation in elastic properties.

It is a significant experimental challenge to design and fabricate an elastically homogeneous, but plastically graded, fully dense alloy with a linear variation in yield strength as a function of depth below the indented surface. Ideally, such a model material system should possess the following attributes:

1. values of Young's modulus and Poisson's ratio should be spatially invariant;
2. the yield strength of the material should vary significantly (and preferably linearly) as a function of depth beneath the indented surface;

*Corresponding author. Tel.: +1 617 253 3320; fax: +1 617 253 0868.
E-mail address: ssuresh@mit.edu (S. Suresh).

0022-5096/$ - see front matter © 2007 Elsevier Ltd. All rights reserved.
doi:10.1016/j.jmps.2007.07.006

3. the processing method employed should provide sufficient flexibility to adjust the thickness of the graded material as compared with the region of elastic deformation surrounding the indenter, for indentations at multiple length scales;
4. the internal interfaces (e.g., grain boundaries or layer interfaces) in the graded material should be sufficiently well bonded so as to avoid brittle fracture in the region of intense deformation surrounding the indenter (since this is likely to offset any potential benefits of mechanical property gradation) and
5. in order to critically assess the experimental trends in light of the predictions reported in Part I, the processing method either should not lead to long-range internal stresses (Suresh and Mortensen, 1998; Suresh, 2001), or the model system and/or test methods employed should be sufficiently quantitative so as to facilitate the separation of any potential effects of residual stresses on the inferred indentation response.

In light of these considerations, the model graded system chosen for direct comparison with the analysis in Part I was a grain size graded nc Ni–W alloy. This choice was motivated by a number of factors. For example, nc metals and alloys (with average and maximum grain size values below 100 nm) can now be produced at full density using a variety of experimental methods (Gleiter, 2000; Kumar et al., 2003; Meyers et al., 2006; Dao et al., 2007). Introducing a gradient in grain size leads to one in yield strength via the classical Hall–Petch effect, but without necessarily requiring a gradient in elastic properties. Furthermore, the strain hardening coefficient of nc metals is essentially zero over a broad range of achievable yield stresses, and consequently, gradients in strain hardening behavior can be minimized as well. Finally, indentation as well as frictional sliding experiments conducted on nc metals point to their relatively stronger resistance to contact damage, especially resistance to crack initiation, as compared to their microcrystalline counterparts (Schuh et al., 2002; Bellemare et al., 2007a, b).

In what follows, we first briefly describe the experimental technique used to synthesize plastically graded Ni–W alloys. To ensure that this material meets the ideal requirements outlined above, we next conduct a detailed evaluation of the mechanical properties as a function of thickness through the specimen. This includes an evaluation of the plastic and elastic properties to justify a proper comparison with—and to parameterize—the computational model of Part I. We conclude with a direct comparison between the experimental and computational indentation response of a plastically graded material, simultaneously validating the modeling approach and material synthesis technique.

2. Preparation of graded Ni–W alloys

With the requirements laid out above in mind, we have worked with a model nc Ni–W system in the present study. Grain size has been graded from ~90 to ~20 nm (resulting in a hardness range of ~4.8 to ~8.3 GPa, respectively) over a 20 μm thickness. This fine level of microstructural control has been realized using a new electrodeposition technique (Detor and Schuh, 2005, 2007).

Nanocrystalline Ni–W alloys processed by electrodeposition exhibit a characteristic relationship between composition and grain size. This relationship is rooted in the thermodynamics of grain boundary segregation: W atoms apparently stabilize grain boundaries, so that increases in W content compel the system to finer grain sizes (Weissmuller, 1993). A key practical consequence of this effect is that grain size can be tailored via judicious control of alloy composition. By tailoring the electrodeposition process to affect the level of W incorporation in growing deposits, grain size can be changed *in situ* to create a graded structure. Moreover, the hardness contrast that can be achieved in this system is quite high, ranging from ~2 to ~9 GPa, while the change in elastic modulus is only of order ~10% and the strain hardening coefficient is uniform and about equal to zero. Thus, the graded specimens produced in this work represent a model system with, at least nominally, a gradient in only the hardness/yield strength, without any appreciable gradients in other mechanical properties.

We note that for comparison with the model in Part I of this paper, a linear spatial gradient in strength is required. Because the Hall–Petch equation is parabolic (i.e., strength increases as the reciprocal square root of grain size), a parabolic grain size profile is required in order to linearly grade strength. This represents a straightforward adaptation of the method presented in Detor and Schuh (2007), which we have implemented here.

A schematic cross-section of the experimental Ni–W alloy used in the present study is presented in Fig. 1(a). This specimen was synthesized using aqueous electrodeposition where a copper substrate served as the cathode, and pure platinum mesh was used as the anode. The temperature of the plating bath was held at a constant 75 °C and the bath composition can be found in Yamasaki et al. (2000). To achieve the required grain size/composition gradient, we used a periodic reverse pulsing technique; a constant forward (cathodic) current density of 0.2 A/cm^2 applied for 20 ms was followed by a 3 ms reverse (anodic) pulse of a particular current density to adjust the composition. For the specimen shown in Fig. 1(a) and (b), a reverse pulse intensity of 0.1 A/cm^2 was introduced into the electrodeposition current to build up the 20 μm layer of 20 nm grain size nearest the substrate. Following this, the reverse pulse was systematically increased in 0.005 A/cm^2 increments to a level of 0.3 A/cm^2 to create a grain size gradient from 20 to 90 nm over the 20 μm surface layer. To ensure the level of property control in this specimen, we have performed detailed validation tests to be further described in Section 4.

In addition to the graded specimen of Fig. 1(a) and (b), we have also produced and tested monolithic specimens of constant grain size and composition through the thickness. Two homogeneous nc specimens of

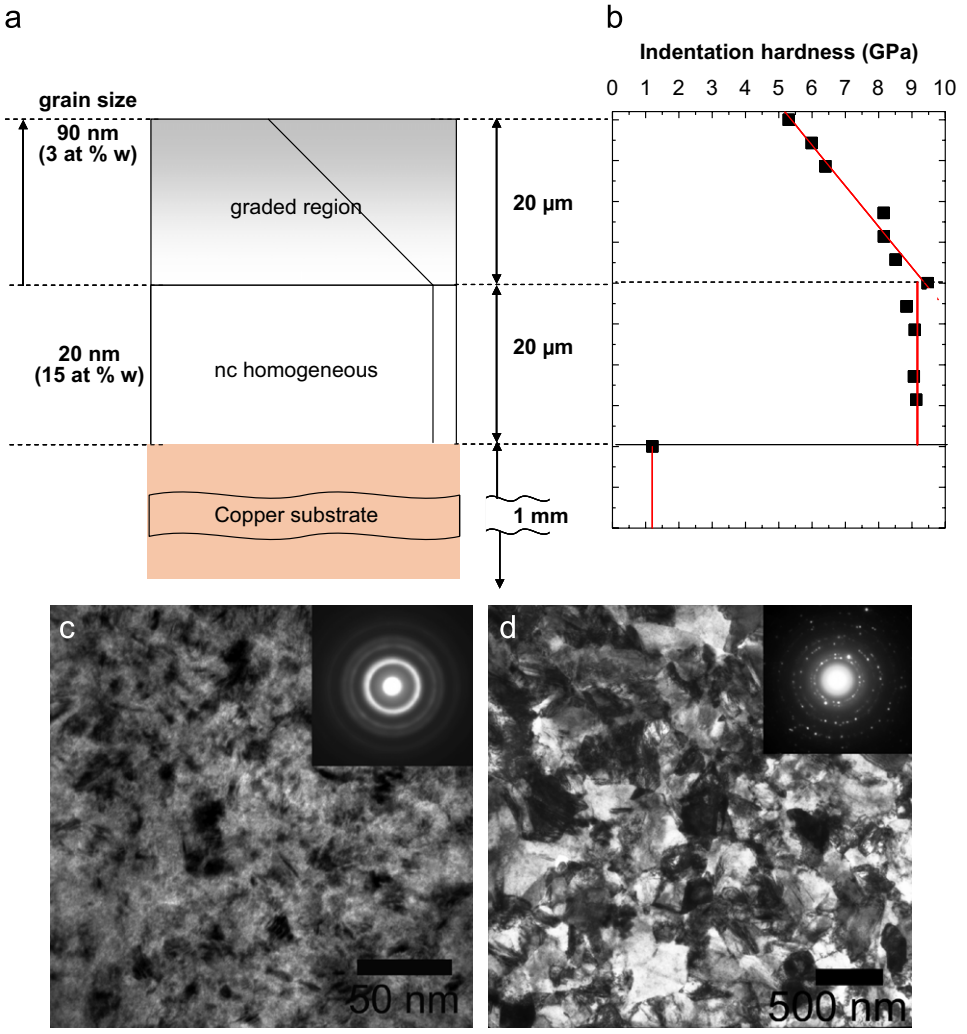

Fig. 1. (a) Schematic cross-section of the graded nanocrystalline Ni–W alloy. A 20 μm thick layer with constant 20 nm grain size and 15 at% W content is followed by a graded region to 90 nm and 3 at% W content on the surface. (b) Indentation hardness profile through the thickness of the graded specimen showing the level of property control. (c and d) Bright field TEM images and selected area diffraction pattern 20 and 90 nm grain size homogeneous Ni–W alloys. (c and d) are taken from Detor and Schuh (2007).

20 and 90 nm grain size were deposited to a thickness of 40 μm as shown in Figs. 1(c) and (d). These homogeneous specimens bound the expected properties of the graded specimen, and will serve as a useful comparison in the analysis that follows.

In preparation for indentation tests, the specimens were mechanically polished using diamond suspensions of 1 and 0.25 μm particle size. Final electropolishing was then conducted in a solution of ethanol, 2-butoxyethanol, perchloric acid, and water in a LectroPol-5 (Struers A/S, Rødovre, Denmark). The electropolishing technique was chosen to avoid work hardening by mechanical polishing, to minimize the removal of material from the graded portion of the specimen (which amounted to ~4 μm), and to give the lowest possible surface roughness. To ensure that the electropolishing did not induce any significant structural changes, we have compared the indentation response of electropolished homogeneous 20 and 90 nm grain size Ni–W specimens with those prepared only by mechanical polishing. The difference in load between these two techniques was found to be small (less than 3%) at depths over 1 μm, which is the range most relevant to the present analysis.

3. Indentation procedure

Indentation experiments were conducted using a Nano Indenter XP (MTS Systems Corporation, Eden Prairie, MN, USA) with a diamond Berkovich tip. The tip radius is about 150 nm, but the effect of tip bluntness is not important since the indentation depth is ~3.5 μm ($\gg$150 nm). This instrument uses a coil-magnet assembly for loading the probe, and measures the displacement into the sample with a capacitance gauge; it is known for its low machine compliance in the high-load range and for precise detection of sample contact. In addition to accurate load and displacement data, the instrument also provides continuous measurement of the contact stiffness via a superimposed AC signal during loading (i.e., the so-called continuous stiffness measurement (CSM) method) so that the indentation hardness and modulus evaluated using the Oliver–Pharr method (Oliver and Pharr, 1992) can be tracked continuously throughout the depth of indentation. With this method, we also develop the means to verify how the hardness of a graded material varies as a function of indentation depth and to compare with the trends predicted in Part I. Further details about this instrument can be found in the literature (Oliver and Pharr, 1992).

For each specimen, at least eight indentations were made to a depth of 4 μm at a constant indentation strain rate of 0.05 s^{-1}. Following this, the load was held constant for 10 s, the tip was unloaded to 10% of the maximum load, held for 50 s in order to determine the displacement rate produced by drift, and finally fully unloaded. The data were subsequently corrected for machine compliance, and also for drift assuming a constant rate throughout the test.

Fig. 2(a) shows a typical indentation geometry using a conical indenter at the maximum indentation depth, h_m, with its corresponding contact radius, a_m. Fig. 2(b) illustrates the residual profile after complete unloading, where h_r is the residual indentation depth, h_p is the pile-up height and a_r is the residual impression radius. The pile-up height h_p is an important parameter that is closely related to the accurate measurement of the indentation impression radius a_r and hardness value. Ignoring the pile-up effect can result in considerable

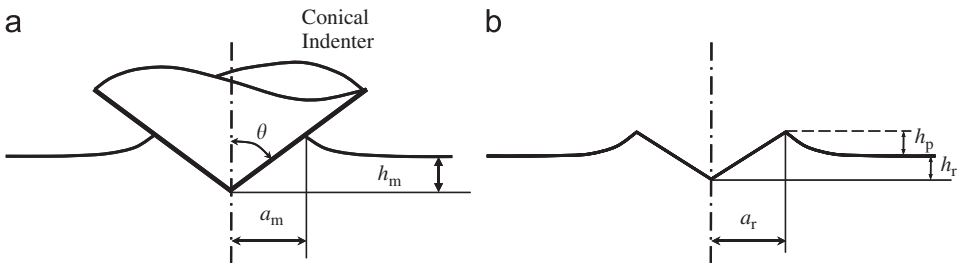

Fig. 2. Schematic drawings and nomenclature of indentation with a conical indenter. (a) Indentation geometry at the maximum indentation depth, h_m, with its corresponding contact radius, a_m. (b) Residual profile after complete unloading, where h_r is the residual indentation depth, h_p is the pile-up height and a_r is the residual impression radius.

errors in extracting mechanical properties from instrumented indentation experiments (Oliver and Pharr, 2004). According to the computational study in Part I, plastically graded materials have unique pile-up behavior as well. The pile-up ratio of h_p/h_r in these materials is a function of the maximum indentation depth h_m, while the pile-up ratio for homogeneous materials is constant during self-similar sharp indentation. Furthermore, the pile-up ratio for the case of an increasing strength gradient is higher than that for the case of the homogeneous material with a surface yield strength equivalent to that of the graded material, which is opposite to the conventional trend. To examine the effect of a plastic gradient on the pile-up of the material around the indenter, high-load conical indentations are required, combined with accurate measurements of the pile-up profile and residual depth. For these experiments, we employed a Micromaterials MicroTest 200 indenter (Micromaterials Ltd., Wrexham, UK) equipped with a diamond conical indenter with a tip apex angle of 70.3° and a tip radius of ~2 μm. Note that this blunted tip is only ~0.125 μm shorter than a perfectly sharp tip at this apex angle, while the maximum indentation depth would be about 20 times the blunted length; the tip can therefore be approximately treated as sharp. For each specimen, at least six indentations were made to a residual indentation depth of about 2.4 μm at a constant indentation strain rate of $0.05\,s^{-1}$. The residual pile-up height (h_p) and residual indentation depth (h_r) were measured using a KLA-Tencor P-10 surface profilometer (KLA-Tencor Corporation, San Jose, California, USA).

4. Mechanical characterization of the graded specimen

Before comparing the experimental indentation response with the computational model presented in Part I of this paper, we first discuss our experiments designed to test the conformity of our specimen to the 'ideal specimen' requirements outlined in the introduction. We first require a continuous and sufficiently large gradient in yield strength normal to the specimen surface, which we have tested by performing indentation hardness tests as a function of thickness through the electrodeposited Ni–W alloy. Typically, the through-thickness gradient is characterized using cross-sectional indentations. Here, however, we take a different approach, where the hardness profile was obtained by first polishing the specimen surface at a slight angle, to reveal a wide, oblique section plane through the Ni–W coating. Normal indents were then made in a series from the surface to the copper substrate. Each indent was performed to a depth of 1 μm and hardness was averaged in the shallow depth range from 400 to 800 nm to achieve as localized a measurement as possible.

Extracting the hardness profile in this way serves a very important purpose in the present work, in the context of managing and interpreting the possible role of residual stress in indentation, as outlined in the introduction. Although we have no data regarding the possible presence or absence of residual stresses in the graded specimen, it is reasonable to assume that if any such residual stresses were present they would be of an in-plane biaxial character (as expected in general for deposited films and coatings). Our hardness measurements, being conducted nearly on the plane normal axis, implicitly incorporate information about biaxial residual stress. Thus, the unknown residual stress state of our specimen (and even any possible gradients in the residual stress state) are naturally accounted for in our measurements; if these are used to calibrate the model from Part I, residual stress is effectively eliminated as a source of error. As an additional benefit, the use of an oblique section also allows for higher resolution of the through-thickness hardness. The resulting hardness profile for the graded specimen is shown in Fig. 1(a) and (b), clear linear trend can be seen with hardness increasing through the sample thickness.

In addition to the hardness profile technique described above, we have also measured hardness continuously using the CSM method; this technique serves as an additional means to confirm the level of property variation through the experimental specimen. Hardness measured using this method is plotted as a function of indentation depth in Fig. 3 for the graded and homogeneous specimens. The hardness of the homogeneous specimens is constant over the full range of indentation depth measuring ~8.3 and ~4.8 GPa for the 20 and 90 nm grain size cases, respectively. Therefore, no indentation size effect for nc Ni–W alloys was observed for grain sizes between 20 and 90 nm in the given indentation range. Note that this is different from cases where the indentation size effect results from geometrically necessary dislocations in larger crystals (Nix and Gao, 1998). The possible deformation mechanisms in nc materials are significantly different from those observed in microcrystalline materials, and they operate at length scales comparable to the grain size (Dao et al., 2007).

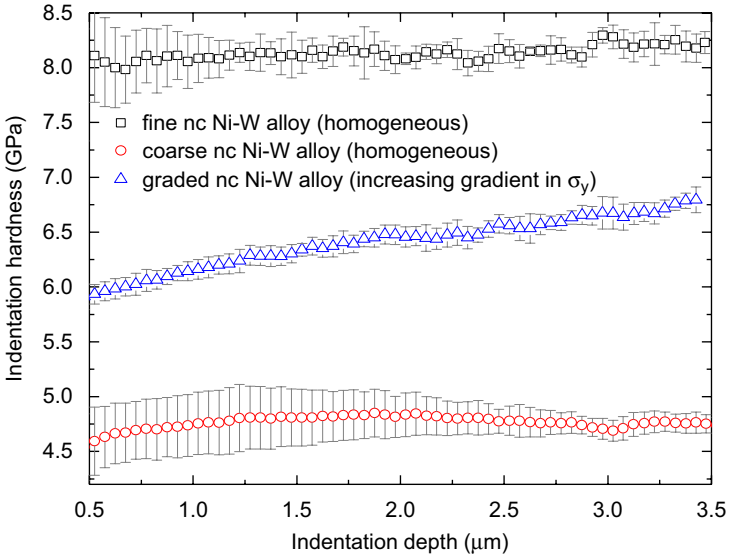

Fig. 3. Indentation hardness vs. indentation depth for the graded and homogeneous nc Ni–W alloys. The fine-grained homogenous alloy maintains a high constant hardness of ~8.3 GPa while the coarse-grained alloy has the lowest hardness of ~4.8 GPa. The hardness of the graded specimen increases with indentation depth between these two extremes.

In the present study, the maximum indentation depth (~3.5 μm) was chosen to be much greater than the experimental grain sizes (less than 100 nm), so it seems reasonable that no indentation size effect is observed.

In contrast to the above results on homogeneous specimens, the graded specimen shows non-self-similar behavior, such that hardness increases with depth as the indenter accesses material of decreasing grain size (note that the surface hardness of the graded specimen is slightly higher than the value for the 20 nm homogeneous case, because some portion of the graded region near the surface was removed during polishing). The measurements presented in Figs. 1(b) and 3 are consistent with one another, and confirm the presence and magnitude of the strength gradient in the experimental specimen.

With characterization of the plastic properties, we now address the additional important point requiring a negligible change in elastic modulus through the graded Ni–W specimen. Using the CSM method we have also measured the Young's modulus (taking Poisson's ratio as 0.3) as a function of indentation depth; the results are presented in Fig. 4. The most important result captured here is that the Young's modulus of the graded specimen is roughly constant through the thickness and, within the scatter of the data, the Young's modulus of all three specimens (homogeneous and graded) is comparable. It is interesting to note, however, that the Young's modulus of the fine-grained specimen (20 nm) having higher W content appears to have a slightly lower modulus than the coarser-grained specimen. To check whether this possible modulus change could have a significant impact on the indentation response, several simulations have been conducted for the various possible extreme cases. Using the FE model setup developed in Part I of this paper (Choi et al., 2007), five load–depth curves are plotted in Fig. 5. The upper and lower curves (blue and cyan, respectively) represent homogeneous fine (20 nm) and coarse (90 nm)-grained Ni–W specimens with constant moduli of 183 and 210 GPa from the mean values of moduli in Fig. 4. The middle red (open circle) and green (open triangle) curves plot the response for the experimentally observed gradient in yield strength with constant modulus of 210 and 183 GPa, respectively. And, finally, the middle black (open square) curve represents a material having both yield strength and modulus gradients. From these computations, we conclude that even the most extreme possible elastic modulus gradient in the experimental material will have a negligible effect on the indentation response; the gradient in plasticity will therefore be the focus in the remainder of this paper.

From the above analysis, the graded nc Ni–W alloy meets the requirements laid out in the Introduction, and can be considered a good model system against which to validate the computational results from Part I of this paper.

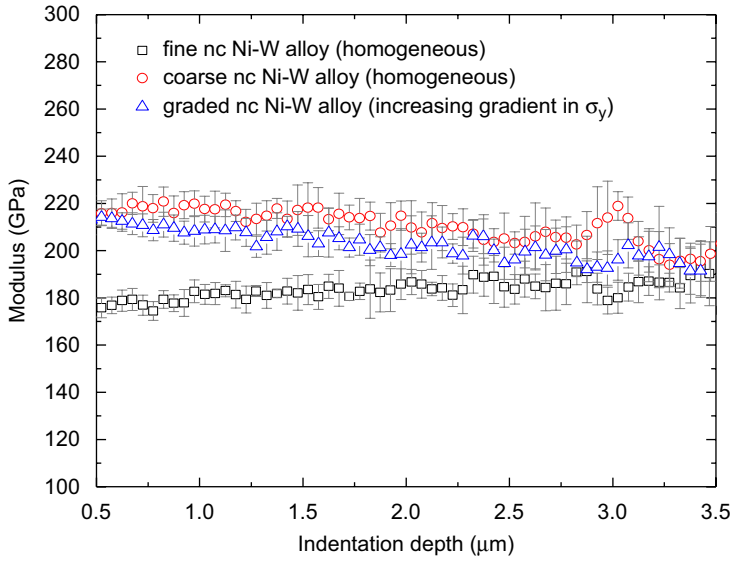

Fig. 4. Elastic modulus vs. indentation depth for the homogeneous and graded Ni–W alloys. The modulus of the graded alloy is roughly constant over the range shown here.

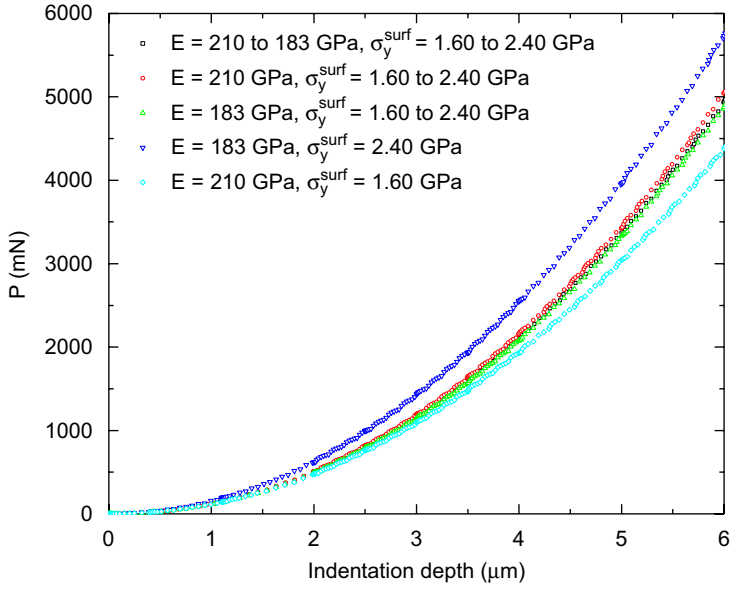

Fig. 5. Computational prediction of the effect of elasticity and plasticity gradients on indentation response. Considering the modulus and hardness variations shown in Figs. 3 and 4, respectively, hardness is found to have the dominant effect.

5. Experiment vs. computation

In this section, we compare the indentation response with that predicted by the computational model of Part I. Before doing so, however, it is essential to establish several model parameters. First, the gradient, β, must be defined which describes the linear gradient in yield strength from the surface as:

$$\sigma_y(Z) = \sigma_y^{surf}(1 + \beta Z). \tag{1}$$

Here, σ_y^{surf} is the yield strength at the surface, and $\sigma_y(Z)$ is the yield strength at a dimensionless distance Z into the material. For $\beta = 0$, the homogeneous case is recovered, while for $\beta > 0$ the yield strength increases with depth, and vice versa. We can simply calculate the value of β as the difference in hardness between the homogeneous coarse-and fine-grained Ni–W specimens over the graded distance of 20 μm in Fig. 1. Alternatively, we can measure the slope of the best-fit line in the graded region of Fig. 1(b). In both cases, the value of β is found to be approximately 0.03684 μm^{-1} and we have used this value in the computational model.

From the analysis in Part I, we derived the dimensionless functional form of mean pressure as

$$\frac{P}{E^* h^2} = \frac{C^*_{dfc}}{E^*}\left[1 - \exp(-(k(\beta h)^d)\right] + \frac{C_H}{E^*}\exp(-(k(\beta h))^d), \tag{2}$$

where P is the load, h the indentation depth, E^* the reduced modulus, k and d are dimensionless constants, and C^*_{dfc} and C_H are the respective indentation curvatures for impression of an elastic-half space and an elasto-plastic homogeneous material with a rigid conical indenter (Choi et al., 2007). The constants k, d, C^*_{dfc} and C_H are, furthermore, all functions of E^*, n (the strain hardening exponent) and/or $\varepsilon^*_y = \sigma_y^{surf}/E^*$ (the strain at yield), as described in Part I of this paper. Modeling the P vs. h response, therefore, further requires values for the constants E^*, n and σ_y^{surf}.

Using the reverse algorithm as introduced by Dao et al. (2001) we can extract the reduced modulus, yield strength and strain hardening exponent from the experimental indentation curve of the homogeneous coarse-grained nc Ni–W specimen. The elasticity of the diamond indenter is taken into account using Young's modulus $E_{in} = 1100$ GPa and Poisson's ratio $\nu_{in} = 0.07$. This analysis yields values of $E^* = 168.6$ GPa ($E_{Ni-W} = 181$ GPa), $\sigma_y = 1.374$ GPa, and $n = 0$; these values are in line with those reported in similar experiments on nc Ni (Schwaiger et al., 2003; Hanlon, 2004; Hanlon et al., 2005). Taking into account the removed surface layer of ~4 μm on the graded specimen after polishing, we estimate the surface yield strength to be $\sigma_y = 1.598$ GPa using the relationship in Eq. (1). With this value and the reduced modulus reported above, ε^*_y evaluates to 9.480×10^{-3}. Using these values and the relations in Part I of this paper, we calculate k, d, C^*_{dfc} and C_H as 0.7466, 0.2670, 316.29, and 111.20, respectively. Since Young's modulus extracted from the reverse algorithm is about 9% lower than the average indentation modulus obtained from the experiment (Fig. 4), we also evaluate ε^*_y using $E^* = 184.9$ GPa corresponding to the average modulus of the graded material ($E = 202$ GPa) in Fig. 4. With the same surface yield strength $\sigma_y = 1.598$ GPa, ε^*_y evaluates to 8.645×10^{-3} and then k, d, C^*_{dfc} and C_H are calculated as 0.7481, 0.2377, 346.85 and 114.55, respectively.

Finally, the effect of friction between the indenter and specimen should be evaluated to accurately model indentation response. This has been investigated in a number of prior studies (Atkinson and Shi, 1989; Shi and Atkinson, 1990; DiCarlo et al., 2004; Mata and Alcala, 2004; Wang and Rokhlin, 2005) with the main result that the friction effect becomes more significant with increasing plasticity contribution (Wang and Rokhlin, 2005). However, since the material system of the present study has a relatively high value of ε^*_y, the friction effect on the indentation force (P) vs. displacement (h) response should be minimal. Indeed, referring to the literature results mentioned above and using our simulation results with a typical friction coefficient of 0.15 (Bellemare et al., 2007a, b), we infer that the maximum difference in indentation curves between a frictional and frictionless condition should be less than 1% in the range of load and displacement of the present case. We can therefore reasonably neglect the contribution of friction to the indentation force (P) vs. displacement (h) response.

Fig. 6 shows experimental indentation load–depth curves for the homogeneous fine- and coarse-grained Ni–W alloys (open squares and circles, respectively) plotted along with the indentation response of the graded specimen (open triangles). As intuitively expected, the graded specimen lies between the two extreme homogeneous cases. Furthermore, the computational predictions from the universal function using $E^* = 168.6$ GPa ($E_{Ni-W} = 181$ GPa) and $E^* = 184.9$ GPa ($E_{Ni-W} = 202$ GPa) are shown in Fig. 6, matching the experimental result within 5% and 2% errors, respectively. The yield strength gradient $\beta = 0.03684\ \mu m^{-1}$, together with $\sigma_y = 1.598$ GPa and $n = 0$, is used in the simulations. Thus, for at least the single case considered here, where there is no strain hardening, the forward analysis algorithms and formulae developed in Part I are found to be reasonably accurate for a plastically graded material. In addition, the two solid lines in Fig. 6 show the predictions using the universal function, obtained by setting the gradient β to zero and assessing the remining input parameters by means of the reverse analysis for homogeneous fine and coarse nc Ni–W

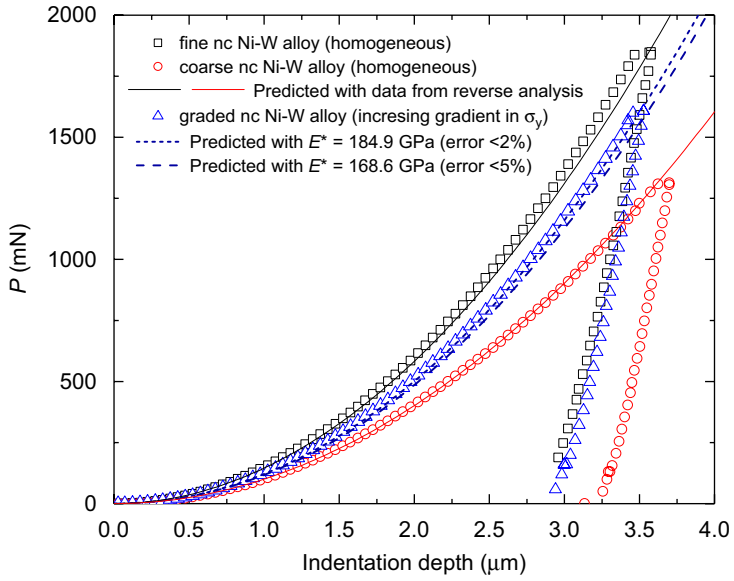

Fig. 6. Indentation response for the homogeneous and graded nc Ni–W specimens. The predictions using the universal function with $E^* = 168.6$ GPa ($E_{Ni-W} = 181$ GPa, long dashed line) and $E^* = 184.9$ GPa ($E_{Ni-W} = 202$ GPa, short dashed line) are plotted, matching the experimental result within 5% and 2% errors, respectively. The yield strength gradient $\beta = 0.03684\,\mu m^{-1}$, together with $\sigma_y = 1.598$ GPa and $n = 0$, is used in the theoretical predictions. The two solid lines are the predictions using the universal function (by setting gradient to zero) with input data obtained from the reverse analysis for homogeneous materials. Error bars for experimental data are comparable to the size of the symbols.

Table 1
Residual indentation depth, h_r, pile-up height, h_p, and pile-up ratio, h_p/h_r, measured experimentally for graded nc Ni–W with an increasing plasticity gradient, coarse nc Ni–W and fine nc Ni–W

	Residual indentation depth h_r (μm)	Pile-up height h_p (μm)	Pile-up ratio h_p/h_r	Error
Graded nc Ni–W	2.39	0.2345	0.0981	0.0232
Coarse nc Ni–W	2.48	0.1275	0.0514	0.0146
Fine nc Ni–W	2.31	0.0754	0.0327	0.0064

materials (with maximum errors of 4% and 1.4%, respectively, vs. the corresponding experimental data points).

The influence of the plastic gradient upon pile-up height was studied using surface profilometry. Table 1 summarizes the residual pile-up height h_p, the residual indentation depth h_r and the pile-up ratio h_p/h_r measured experimentally. The residual indentation depth h_r was chosen as the maximum value from among the scanned profiles, and at least 10–14 scanned profiles were used to determine the averaged pile-up height h_p for each case. Fig. 7 compares the experimentally measured pile-up ratios with the results computed using finite-element methods (FEM) with or without friction. The case with friction used a typical friction coefficient of $f = 0.15$. The plastically graded material is the nc Ni–W alloy with increasing gradient in σ_y, the surface material is the homogeneous coarse nc Ni–W alloy with 90 nm grain size, and the "back-surface" material is the homogeneous fine nc Ni–W alloy with 20 nm grain size. Fig. 7(a) compares values of the obtained ratio h_p/h_r, where the experiments as well as the FEM results all show that the pile-up for the plastically graded material (from coarse to fine nc Ni–W) is higher than both the surface material (coarse nc Ni–W) or the back-surface material (fine nc Ni–W). This confirms the general trend discussed in Part I based on computational simulations (Choi et al., 2007). What is perhaps more significant is the relative trend in pile-up behavior among the three specimens; this is examined in Fig. 7(b) by plotting the pile-up ratio normalized to that

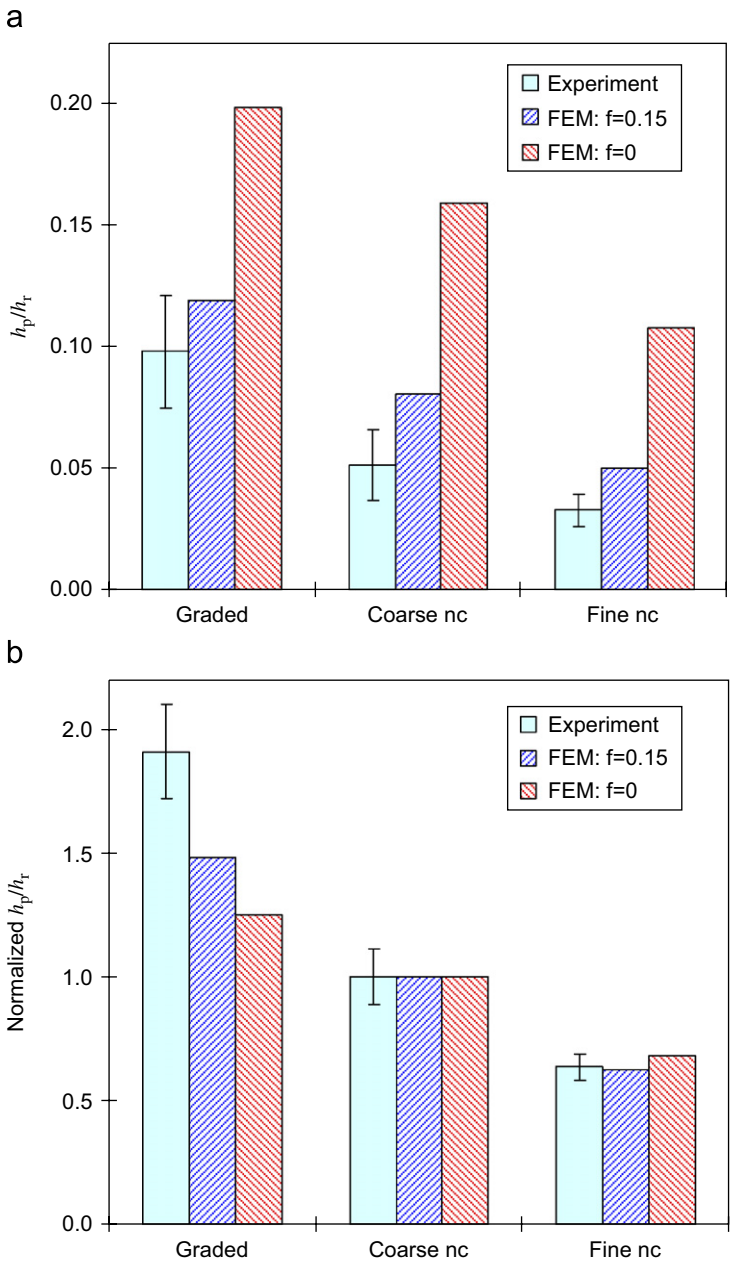

Fig. 7. Residual pile-up height measured experimentally and computed using FEMs with or without friction at the interface between the indenter and the specimen. The plastically graded material is the nc Ni–W alloy with increasing gradient in σ_y, the surface material is the homogeneous coarse nc Ni–W alloy with 90 nm grain size, and the back-surface material is the homogeneous fine nc Ni–W alloy with 20 nm grain size. (a) Direct comparison of the ratio h_p/h_r. (b) Comparison of the ratio h_p/h_r normalized to that of the surface coarse nc Ni–W material.

obtained for the surface material. Here, we now see more directly the effect of the plastic gradient in promoting pile-up, and the fact that this relative trend is captured well by the FEM calculations.

A final interesting finding illustrated in Fig. 7 is that, although friction has little effect on the P–h response, it does have significant influence on the pile-up height. When the frictional force is considered, the FEM results are reasonably close to the experimental observations. As discussed in Marx and Balke (1997), Cheng

and Cheng (1998) and Bellemare et al. (2007a, b), the strain hardening exponent also has a strong influence on the pile-up height. This is one possible factor contributing to the discrepancies between the experimental and the computational results. Nevertheless, the relative trends for all cases are very consistent, as seen in Fig. 7(b).

6. Conclusions

In the present work, the experimental indentation response of a plastically graded nc alloy has been directly compared with the prediction of a computational model. The requirements of a suitable experimental material with which to perform this validation have been presented, leading to the development of a graded nc alloy, where a grain size gradient has been used to vary strength. Through detailed analysis of through-thickness properties we have confirmed that the experimental specimen exhibits ideal plastically graded behavior, showing a clear linear trend in hardness with negligible change in elastic modulus. After calibrating the unknown constants in the dimensionless function for linearly graded plastic material presented in Part I of this paper, the experimental and computation indentation load–depth curves as well as normalized pile-up ratios were found to exhibit excellent agreement.

Acknowledgments

This research was supported by the Defense University Research Initiative on Nano-Technology (DURINT) on "Damage and Failure Resistant Nanostructured Materials" which is funded at MIT by the Office of Naval Research, Grant no. N00014-01-1-0808, and by a Grant to MIT from the Schlumberger-Doll Company. CAS and AJD were supported by the US Army Research Office, under Grant DAAD19-03-1-0235. CAS also acknowledges the support of the US National Science Foundation, under Grant DMI-0620304.

References

Atkinson, M., Shi, H., 1989. Friction effect in low load hardness testing of iron. Mater. Sci. Technol. 5 (6), 613–614.

Bellemare, S., Dao, M., Suresh, S., 2007a. The frictional sliding response of elasto-plastic materials in contact with a conical indenter. Int. J. Solids Struct. 44 (6), 1970–1989.

Bellemare, S., Dao, M., Suresh, S., 2007b. Effects of mechanical properties and surface friction on elasto-plastic sliding contact. Mech. Mater., in press.

Cheng, Y.T., Cheng, C.M., 1998. Effects of 'sinking in' and 'piling up' on estimating the contact area under load in indentation. Philos. Mag. Lett. 78 (2), 115–120.

Choi, I.S., Dao, M., Suresh, S., 2007. Indentation of plastically graded materials: I. Analysis. J. Mech. Phys. Solids, in press. doi:10.1016/j.jmps.2007.07.007.

Dao, M., Chollacoop, N., Van Vliet, K.J., Venkatesh, T.A., Suresh, S., 2001. Computational modeling of the forward and reverse problems in instrumented sharp indentation. Acta Mater. 49 (19), 3899–3918.

Dao, M., Lu, L., Asaro, R.J., De Hosson, J.T.M., Ma, E., 2007. Toward a quantitative understanding of mechanical behavior of nanocrystalline metals. Acta Mater. 55 (12), 4041–4065.

Detor, A.J., Schuh, C.A., 2005. Method for Producing Alloy Deposits and Controlling the Nanostructure Thereof Using Negative Current Pulsing Electrodeposition, and Articles Incorporating Such Deposits. US Patent Application #11/147,146.

Detor, A.J., Schuh, C.A., 2007. Tailoring and patterning the grain size of nanocrystalline alloys. Acta Mater. 55 (1), 371–379.

DiCarlo, A., Yang, H.T.Y., Chandrasekar, S., 2004. Prediction of stress–strain relation using cone indentation: effect of friction. Int. J. Numer. Methods Eng. 60 (3), 661–674.

Gleiter, H., 2000. Nanostructured materials: basic concepts and microstructure. Acta Mater. 48 (1), 1–29.

Hanlon, T., 2004. Grain Size Effects on the Fatigue Response of Nanocrystalline Materials. Deptartment of Materials Science and Engineering, Cambridge, MIT.

Hanlon, T., Tabachnikova, E.D., Suresh, S., 2005. Fatigue behavior of nanocrystalline metals and alloys. Int. J. Fatigue 27 (10–12), 1147–1158.

Kumar, K.S., Van Swygenhoven, H., Suresh, S., 2003. Mechanical behavior of nanocrystalline metals and alloys. Acta Mater. 51 (19), 5743–5774.

Marx, V., Balke, H., 1997. A critical investigation of the unloading behavior of sharp indentation. Acta Mater. 45 (9), 3791–3800.

Mata, M., Alcala, J., 2004. The role of friction on sharp indentation. J. Mech. Phys. Solids 52 (1), 145–165.

Meyers, M.A., Mishra, A., Benson, D.J., 2006. Mechanical properties of nanocrystalline materials. Prog. Mater. Sci. 51 (4), 427–556.

Nix, W.D., Gao, H.J., 1998. Indentation size effects in crystalline materials: a law for strain gradient plasticity. J. Mech. Phys. Solids 46 (3), 411–425.

Oliver, W.C., Pharr, G.M., 1992. An improved technique for determining hardness and elastic-modulus using load and displacement sensing indentation experiments. J. Mater. Res. 7 (6), 1564–1583.
Oliver, W.C., Pharr, G.M., 2004. Measurement of hardness and elastic modulus by instrumented indentation: advances in understanding and refinements to methodology. J. Mater. Res. 19 (1), 3–20.
Schuh, C.A., Nieh, T.G., Yamasaki, T., 2002. Hall-Petch breakdown manifested in abrasive wear resistance of nanocrystalline nickel. Scripta Mater. 46 (10), 735–740.
Schwaiger, R., Moser, B., Dao, M., Chollacoop, N., Suresh, S., 2003. Some critical experiments on the strain-rate sensitivity of nanocrystalline nickel. Acta Mater. 51 (17), 5159–5172.
Shi, H., Atkinson, M., 1990. A friction effect in low-load hardness testing of copper and aluminum. J. Mater. Sci. 25 (4), 2111–2114.
Suresh, S., 2001. Graded materials for resistance to contact deformation and damage. Science 292 (5526), 2447–2451.
Suresh, S., Mortensen, A., 1998. Fundamentals of Functionally Graded Materials. Institute of Materials, London.
Wang, L., Rokhlin, S.I., 2005. Universal scaling functions for continuous stiffness nanoindentation with sharp indenters. Int. J. Solids Struct. 42 (13), 3807–3832.
Weissmuller, J., 1993. Alloy effects in nanostructures. Nanostruct. Mater. 3 (1–6), 261–272.
Yamasaki, T., Tomohira, R., Ogino, Y., Schlossmacher, P., Ehrlich, K., 2000. Formation of ductile amorphous & nanocrystalline Ni–W alloys by electrodeposition. Plat. Surf. Finish. 87 (5), 148–152.